International Journal of Thermophysics, Vol. 20, No. 5, 1999

Vapor–Liquid Critical Surface of Ternary Difluoromethane + Pentafluoroethane + 1,1,1,2-Tetrafluoroethane (R-32/125/134a) Mixtures

Y. Higashi[1]

Received December 28, 1998

The plane of vapor–liquid criticality for ternary refrigerant mixtures of difluoromethane (R-32) + pentafluoroethane (R-125) + 1,1,1,2-tetrafluoroethane (R-134a) was determined from data on the vapor–liquid coexistence curve near the mixture critical points. The compositions (mass percentage) of the mixtures studied were 23% R-32 + 25% R-125 + 52% R-134a (R-407C), 25% R-32 + 15% R-125 + 60% R-134a (R-407E), and 20% R-32 + 40% R-125 + 40% R-134a (R-407A). The critical temperature of each mixture was determined by observation of the disappearance of the meniscus. The critical density of each mixture was determined on the basis of meniscus disappearance level and the intensity of the critical opalescence. The uncertainties of the temperature, density, and composition measurements are estimated as ± 10 mK, $\pm 5\ \mathrm{kg \cdot m^{-3}}$, and ± 0.05%, respectively. In addition, predictive methods for the critical parameters of R-32/125/134a mixtures are discussed.

KEY WORDS: critical properties; R-32/125/134a; R-407A; R-407C; R-407E; saturated densities; vapor–liquid coexistence curve.

1. INTRODUCTION

Because of their low ozone-depletion potentials, hydrofluorocarbon (HFC) mixtures are used as the working fluid in air-conditioning and heat-pump systems. Ternary refrigerant mixtures of difluoromethane (R-32) + pentafluoroethane (R-125) + 1,1,1,2-tetrafluoroethane (R-134a), i.e., R-32/125/134a, are candidates for replacing chlorodifluoromethane (R-22). However, reliable information on the thermophysical properties of this mixture is limited.

[1] Department of Mechanical Engineering, Iwaki Meisei University, 5-5-1, Iino, Chuodai, Iwaki 970-8551, Japan.

0195-928X/99/0900-1483$16.00/0

The author has already measured the isothermal vapor–liquid equilibrium and vapor–liquid coexistence curve for the R-32/134a mixture [1], the R-32/125 mixture [2], and the R-125/134a mixture [3] and has proposed a correlation for the critical loci of these three binary mixtures. In this paper, measurements of vapor–liquid coexistence curves and determination of points on the critical plane of the ternary mixture R-32/125/134a are reported. Moreover, predictive methods for the critical parameters of ternary mixtures are discussed.

2. EXPERIMENTAL APPARATUS AND PROCEDURES

Measurements of the vapor–liquid coexistence curve near the critical point were carried out based on the observation of meniscus disappearance. The author has already described in detail the experimental apparatus at Iwaki Meisei University [4]. The main portion of the apparatus is composed of three pressure vessels, that is, an optical cell with two Pyrex windows, an expansion vessel used to change the sample density in the optical cell without a new sample charge, and a supply vessel used to change the sample density and prepare the initial sample mixture. The apparatus was installed in a thermostated silicone oil bath. The bath temperature could be kept constant within a temperature fluctuation of ± 5 mK. Temperature measurements were made with a thermometer bridge using a 25-Ω standard platinum resistance thermometer calibrated on ITS-90. The thermometer was mounted in close proximity to the optical cell. The uncertainty of temperature measurements is estimated to be within ± 10 mK.

The sample density in the optical cell can be calculated from the mass of the sample and the interior volume of the three vessels. An expansion procedure was introduced in the present measurements in order to change the sample density in the optical cell. The uncertainty of the density measurements is different for each measurement in this work. It is unavoidable that the experimental uncertainty in the density measurements is directly proportional to the total number of expansion steps. The number of expansion steps was restricted to maintain an uncertainty of density measurement within $\pm 0.5\%$.

For preparation of the sample mixture with a prescribed density and composition, additional pressure vessels were used. Each vessel was filled with the appropriate pure components and weighed on a precision chemical balance with an uncertainty of ± 2 mg. Whenever the targeted amount for a given component was exceeded, some of the component was discharged. Each component was then transferred to the supply vessel evacuated to 0.5 mPa and cooled by liquid nitrogen. It was estimated that

the uncertainty of the mass of the sample thus obtained was not greater than ±0.1%. In addition, the uncertainty of the composition of the sample was estimated to be within ±0.05%. In this experiment, a gas chromatograph was not used to determine compositions.

The samples of pure R-32, R-125, and R-134a had stated sample purities of 99.99 mass% R-32, 99.99 mass% R-125, and 99.99 mass% R-134a. These samples were used without further purification.

3. RESULTS

3.1. Vapor–Liquid Coexistence Curve

Vapor–liquid coexistence curves for R-32/125/134a mixtures near the critical plane were measured for several compositions: 23/25/52 mass% R-32/125/134a (R-407C), 25/15/60 mass% R-32/125/134a (R-407E), and 20/40/40 mass% R-32/125/134a (R-407A). The experimental data for R-407C, R-407E, and R-407A are given in Tables I through III, respectively. Tables I through III include the uncertainty of density measurements for each experimental point because the uncertainty of density measurements

Table I. Vapor–Liquid Coexistence Curve of 23.00 Mass% R-32 + 25.00 Mass% R-125 + 52.00 Mass% R-134a (R-407C) Near the Critical Point

T (K)	ρ ($kg \cdot m^{-3}$)
352.213	227.9 ± 1.4
357.339	290.6 ± 1.2
358.018	319.1 ± 1.7
358.877	366.3 ± 1.2
359.277	402.2 ± 1.6
359.360	459.7 ± 1.5[a]
359.274	501.6 ± 1.6[a]
359.194	513.0 ± 0.9[a]
358.900	563.3 ± 1.8
357.806	627.0 ± 0.6
357.305	646.6 ± 0.6
354.901	710.0 ± 1.2
348.911	810.1 ± 0.8
348.878	811.8 ± 0.8
341.953	886.1 ± 0.8
341.064	895.4 ± 0.9

[a] Critical opalescence was observed.

Table II. Vapor–Liquid Coexistence Curve of 24.99 Mass % R-32 + 15.00 Mass % R-125 + 60.01 Mass % R-134a (R-407E) Near the Critical Point

T (K)	ρ ($kg \cdot m^{-3}$)
358.032	283.4 ± 0.9
361.644	360.9 ± 1.1
362.159	402.8 ± 0.6
361.568	498.4 ± 0.4^a
361.512	507.7 ± 0.4^a
361.518	520.7 ± 0.4^a
361.266	596.7 ± 1.0
360.950	633.2 ± 0.5
360.596	637.1 ± 0.5
358.880	690.4 ± 1.1
355.836	752.1 ± 0.6
345.724	870.6 ± 0.7

[a] Critical opalescence was observed.

depends on the number of expansions. The uncertainty of temperature measurements was estimated to be ± 10 mK.

The experimental results for the vapor–liquid coexistence curves of R-407C, R-407E, and R-407A are shown in Fig. 1, including data for the pure components reported previously [4]. In the temperature–density diagram, all of the present data for R-407C, R-407E, and R-407A are located between the vapor–liquid coexistence curve for pure R-32 and that for pure R-134a. The coexistence curve of R-407E lies at a slightly higher temperature than those of R-407C and of R-407A. This is because the

Table III. Vapor–Liquid Coexistence Curve of 20.00 Mass % R-32 + 40.00 Mass % R-125 + 40.00 Mass % R-134a (R-407A) Near the Critical Point

T (K)	ρ ($kg \cdot m^{-3}$)
354.881	511.0 ± 0.4^a
354.950	517.9 ± 0.4^a
354.867	527.5 ± 0.4^a

[a] Critical opalescence was observed.

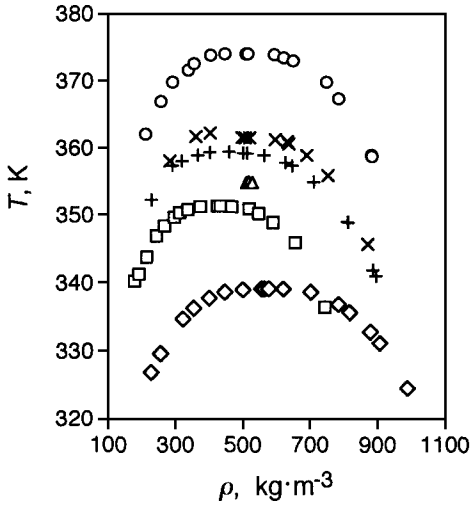

Fig. 1. Vapor–liquid coexistence curve near the critical point for the R-32/125/134a mixtures. (□) R-32; (◇) R-125; (○) R-134a; (+) R-407C; (×) R-407E; (△) R-407A.

amount of R-134a in R-407E is larger than for R-407C and R-407A, and the amount of R-125 in R-407E is less than in R-407C and R-407A.

The asterisks in Tables I through III indicate that critical opalescence was observed at these conditions. There is no special intensity difference of the critical opalescence in these ternary mixtures compared with the pure refrigerants or their binary mixtures.

3.2. Critical Point for R-407C

As in a pure fluid, the critical point of a mixture can be defined as the point at which the meniscus disappears at the center level in an optical cell of constant volume at constant composition. Moreover, the critical point can also be defined as the point at which the critical opalescence of the liquid phase is observed as intensely as that in the vapor phase just before the meniscus disappears. In the present observation of meniscus disappearance for R-407C, the critical opalescence was observed at three densities; 459.7 $kg \cdot m^{-3}$ at 359.360 K, 501.6 $kg \cdot m^{-3}$ at 359.274 K, and 513.0 $kg \cdot m^{-3}$ at 359.194 K. The meniscus at the density 459.7 $kg \cdot m^{-3}$ descended with increasing temperature and disappeared at the bottom of the optical cell. The meniscus at the density 501.6 $kg \cdot m^{-3}$ descended with increasing temperature but disappeared prior to reaching the bottom of the

optical cell, whereas the meniscus at the density 513.0 $kg \cdot m^{-3}$ ascended with increasing temperature but disappeared prior to reaching the top of the optical cell.

Based on these observations of meniscus disappearance, the critical density ρ_c for R-407C was experimentally determined as

$$\rho_c = 506 \pm 5 \text{ kg} \cdot \text{m}^{-3} \tag{1}$$

The critical temperature T_c can be determined as the temperature along the coexistence curve corresponding to the critical density. From the data in Table I and the critical density determined in this study, the critical temperature T_c for R-407C was determined as

$$T_c = 359.23 \pm 0.03 \text{ K} \tag{2}$$

3.3. Critical Point for R-407E

In R-407E, the critical opalescence was observed at three densities: 498.4 $kg \cdot m^{-3}$ at 361.568 K, 507.7 $kg \cdot m^{-3}$ at 361.512 K, and 520.7 $kg \cdot m^{-3}$ at 361.518 K. The meniscus at the density 498.4 $kg \cdot m^{-3}$ descended with increasing temperature but disappeared prior to reaching the bottom of the optical cell. At this density, the intensity of the critical opalescence in the liquid phase was observed to be stronger than that in the vapor phase. The meniscus at the density 520.7 $kg \cdot m^{-3}$ ascended with increasing temperature but disappeared prior to reaching the top of the optical cell. At this density, the intensity of the critical opalescence in the vapor phase was observed to be stronger than that in the liquid phase. At the density 507.7 $kg \cdot m^{-3}$, the meniscus level was unchanged at the center of the optical cell with increasing temperature and finally, disappeared at that level.

Based on these observations of the meniscus disappearance, the critical density ρ_c for R-407E was experimentally determined as

$$\rho_c = 508 \pm 5 \text{ kg} \cdot \text{m}^{-3} \tag{3}$$

The critical temperature T_c for R-407E was determined as the saturation temperature corresponding to the critical density,

$$T_c = 361.51 \pm 0.02 \text{ K} \tag{4}$$

3.4. Critical Point for R-407A

For R-407A, the critical opalescence was observed at three densities: 511.0 $kg \cdot m^{-3}$ at 354.881 K, 517.9 $kg \cdot m^{-3}$ at 354.950 K, and 527.5 $kg \cdot m^{-3}$

at 354.867 K. The meniscus at the density 511.0 $kg \cdot m^{-3}$ descended with increasing temperature and disappeared at the bottom of the optical cell. The meniscus at 517.9 $kg \cdot m^{-3}$ descended with increasing temperature but disappeared prior to reaching the bottom of the optical cell. At this density, the intensity of the critical opalescence in the liquid phase was stronger than that in the vapor phase. At the density 527.5 $kg \cdot m^{-3}$, the meniscus level with increasing temperature was unchanged at the center of the optical cell and finally disappeared at that level. The meniscus reappearance level was at the center of the optical cell at this density.

Based on these observations of meniscus disappearance, the critical density ρ_c and critical temperature T_c for R-407E were experimentally determined as

$$\rho_c = 528 \pm 5 \text{ kg} \cdot \text{m}^{-3} \tag{5}$$

and

$$T_c = 354.87 \pm 0.02 \text{ K} \tag{6}$$

4. DISCUSSION

4.1. Comparison with Critical Points Determined by Nagel and Bier [5]

Experimental data on the critical surface for R-32/125/134a mixtures by Nagel and Bier [5] are available. They measured the critical temperature, critical pressure, and critical molar volume of three R-32/125/134a mixtures: 19.10/43.32/37.58 mass% R-32/125/134a (nearly R-407A), 9.76/70.58/19.66 mass% R-32/125/134a (nearly R-407B), and 27.21/12.69/60.10 mass% R-32/125/134a (nearly R-407C). The critical temperatures and critical molar volumes determined here and those by Nagel and Bier are summarized in Table IV.

The measurements by Nagel and Bier were carried out on three R-32/125/134a mixtures with approximately equal molar amounts of R-32 and R-134a. As a result of this, the compositions they measured are close to R-407A, R-407B, and R-407C. For the composition close to R-407A (20/40/40 mass% R-32/125/134a), the critical temperature of the mixture determined in this study is in good agreement with that by Nagel and Bier. Although the present critical temperature, 354.87 K, is a little higher that of than Nagel and Bier, 354.03 K, it is because the proportion of R-134a in the present mixture is larger than that for the composition of Nagel and Bier.

Table IV. Critical Temperatures and Critical Densities of the R-32/125/134a Mixtures[a]

Mass fraction			Mole fraction			T_c	ρ_c	
w_1	w_2	w_3	x_1	x_2	x_3	(K)	(kg·m^{-3})	Ref.
0.2000	0.4000	0.4000	0.3464	0.3003	0.3533	354.87 ± 0.02	528 ± 5	Present work
0.1910	0.4332	0.3758	0.3349	0.3292	0.3359	354.03 ± 0.06	511 ± 10	Nagel and Bier [5]
0.0976	0.7058	0.1966	0.1938	0.6072	0.1990	347.26 ± 0.06	537 ± 11	Nagel and Bier [5]
0.2300	0.2500	0.5200	0.3811	0.1796	0.4393	359.23 ± 0.03	506 ± 5	Present work
0.2499	0.1500	0.6001	0.4026	0.1047	0.4927	361.51 ± 0.02	508 ± 5	Present work
0.2721	0.1269	0.6010	0.4295	0.0868	0.4837	361.56 ± 0.06	485 ± 10	Nagel and Bier[5]

[a] The following refrigerant numbers are adopted for R-32/125/134a mixtures by ASHRAE: R-407A (20/40/40 mass% R-32/125/134a); R-407B (10/70/20 mass% R-32/125/134a); R-407C (23/25/52 mass% R-32/125/134a); R-407E (25/15/60 mass% R-32/125/134a).

The critical point of R-407C was also measured by Nagel and Bier. The composition of the measurements by Nagel and Bier, 27.21/12.69/60.10 mass% R-32/125/134a, seems to be closer to R-407E than R-407C. The critical temperature of R-407E (24.99/15.00/60.01 mass% R-32/125/134a) determined in this study and that of R-407C by Nagel and Bier (27.21/12.69/60.10 mass% R-32/125/134a) are in good agreement. Although there is a small difference in the critical temperature of R-407C between this study and that by Nagel and Bier, it can be explained since the proportion of R-134a in the present mixture is smaller than that in the mixture of Nagel and Bier.

With respect to the critical density of mixtures, the present results are slightly higher than those of Nagel and Bier. However, the data of Nagel and Bier have a larger uncertainty in the critical density than the present work. Moreover, there are composition differences between the mixtures of the present work and those of Nagel and Bier. Therefore, it is considered that both determinations of the mixture critical density are in reasonable agreement.

4.2. Application of a Predictive Method Using Simple Mixing Rules

Using the present critical parameters of ternary R-32/125/134a mixtures, simple mixing rules are examined for the prediction of the critical temperature and critical molar volume. The functional forms examined are

Table V. Comparisons of the Critical Temperature for R-32/125/134a Mixtures Between Experimental Results and Predictive Results from Eq. (7)[a]

Mixture	$T_{c\,exp}$ (K)	$T_c(w)$ (K)[b]	$T_{c\,exp} - T_c(w)$ (K)	$T_c(x)$ (K)[b]	$T_{c\,exp} - T_c(x)$ (K)	$T_c(\theta)$ (K)[b]	$T_{c\,exp} - T_c(\theta)$ (K)
R-407A	354.87	355.56	−0.69	355.70	−0.83	356.05	−1.18
NB-A	354.03	354.61	−0.58	354.96	−0.93	355.20	−1.17
NB-B	347.26	347.22	0.04	348.47	−1.21	348.17	−0.91
R-407C	359.23	360.12	−0.89	359.13	0.10	359.98	−0.75
R-407E	361.51	363.16	−1.69	361.25	0.26	362.47	−0.96
NB-C	361.56	363.46	−1.90	361.26	0.30	362.59	−1.03
Bias			−0.94		−0.38		−1.00
SD			0.72		0.68		0.17

[a] To simplify the table, the following descriptions of the mixtures measured by Nagel and Bier [5] are used: NB-A, 0.1910 R-32 + 0.4332 R-125 + 0.3758 R-134a in mass fraction; NB-B, 0.0976 R-32 + 0.7058 R-125 + 0.1966 R-134a in mass fraction; and NB-C, 0.2721 R-32 + 0.1269 R-125 + 0.6010 R-134a in mass fraction.

[b] w, mass fraction; x, mole fraction; θ, surface fraction.

$$T_{cm} = \sum_i X_i T_{ci} \tag{7}$$

$$V_{cm} = \sum_i X_i V_{ci} \tag{8}$$

Here T_{cm} denotes the critical temperature and V_{cm} the critical molar volume of the mixture. T_{ci} denotes the critical temperature and V_{ci} the critical molar volume of the pure components. X_i represents the composition. In this study, three composition units are examined: mass fraction w_i, mole fraction x_i, and surface fraction θ_i. The critical parameters for the three pure components that the present author reported previously [4] were adopted. Comparisons between the experimental critical parameters and the predictive models are summarized in Tables V and VI.

For the critical temperatures of R-32/125/134a mixtures, the predictive method using mole fractions gave good results, although the deviations are between +0.30 K and −1.21 K. With respect to the critical molar volume, the predictive method using mole fractions also gave better results than the others.

4.3. Proposal of a Predictive Method for Ternary Refrigerant Mixtures

The author has already proposed correlations for the critical lines of the three binary refrigerant mixtures: R-32/134a [1], R-32/125 [2], and R-125/134a [3]. The functional forms are

Table VI. Comparisons of the Critical Molar Volume for R-32/125/134a Mixtures Between Experimental Results and Predictive Results from Eq. (8)[a]

Mixture	$V_{c\,exp}$ ($cm^3 \cdot mol^{-1}$)	$V_c(w)$ ($cm^3 \cdot mol^{-1}$)	$V_{c\,exp} - V_c(w)$ ($cm^3 \cdot mol^{-1}$)	$V_c(x)$ ($cm^3 \cdot mol^{-1}$)	$V_{c\,exp} - V_c(x)$ ($cm^3 \cdot mol^{-1}$)	$V_c(\theta)$ ($cm^3 \cdot mol^{-1}$)	$V_{c\,exp} - V_c(\theta)$ ($cm^3 \cdot mol^{-1}$)
R-407A	170.7	187.9	−17.2	175.6	−4.9	181.7	−11.0
NB-A	178.5	188.8	−10.3	176.7	1.8	182.7	−4.2
NB-B	192.3	198.2	−5.9	189.9	2.4	194.0	−1.7
R-407C	170.4	184.4	−14.1	172.0	−1.6	178.2	−7.8
R-407E	164.9	182.1	−17.2	169.7	−4.8	176.0	−11.1
NB-C	169.3	180.2	−10.9	167.5	1.8	173.9	−4.6
Bias			−12.6		−0.9		−6.7
SD			4.4		3.4		3.9

[a] Mixture and unit designations as in Table V.

$$T_{cm} = \theta_1 T_{c1} + \theta_2 T_{c2} + 2\theta_1 \theta_2 \Delta_T \tag{9}$$

$$V_{cm} = \theta_1 V_{c1} + \theta_2 V_{c2} + 2\theta_1 \theta_2 \Delta_V \tag{10}$$

$$\rho_{cm} = M_m / V_{cm} \tag{11}$$

$$P_{cm} = \theta_1 P_{c1} + \theta_2 P_{c2} + 2\theta_1 \theta_2 \Delta_P \tag{12}$$

$$\theta_i = \frac{x_i V_{ci}^{2/3}}{\sum_j x_j V_{cj}^{2/3}} \tag{13}$$

Here T_{cm} denotes the critical temperature, V_{cm} the critical molar volume, ρ_{cm} the critical density, and P_{cm} the critical pressure of the binary mixture. M_m denotes the molar mass of the binary mixture, and $M_m = x_1 M_1 + (1 - x_1) M_2$. The surface fraction θ_i is defined in Eq. (13) in terms of composition and the critical molar volumes of the pure components. Δ_T in Eq. (9), Δ_V in Eq. (10), and Δ_P in Eq. (12) are adjustable parameters listed in Table VII.

In order to extend Eqs. (9), (10), and (12) for binary mixtures to the ternary R-32/125/134a mixture, a simple functional form using the critical temperature and critical molar volume was applied. For R-32/125/134a mixtures, extended correlations of the critical temperature and critical molar volume are represented by

$$T_{cm} = \theta_1 T_{c1} + \theta_2 T_{c2} + \theta_3 T_{c3} + 2\theta_1 \theta_2 \Delta_{T12} + 2\theta_2 \theta_3 \Delta_{T23} + 2\theta_3 \theta_1 \Delta_{T31} \tag{14}$$

$$V_{cm} = \theta_1 V_{c1} + \theta_2 V_{c2} + \theta_3 V_{c3} + 2\theta_1 \theta_2 \Delta_{V12} + 2\theta_2 \theta_3 \Delta_{V23} + 2\theta_3 \theta_1 \Delta_{V31} \tag{15}$$

Subscripts 1, 2, and 3 denote the pure components of R-32, R-125, and R-134a, respectively. Moreover, subscripts 12, 23, and 31 denote the binary mixtures of R-32/125, R-125/134a, and R-32/134a, respectively. The purpose of Eqs. (14) and (15) is to be able to calculate the critical parameters of not only ternary mixtures but also of pure components and binary

Table VII. Adjustable Parameters Δ_T in Eq. (9), Δ_V in Eq. (10), and Δ_P in Eq. (12) for the Binary Mixtures R-32/134a, R-32/125, and R-125/134a

	Δ_T (K)	Δ_V ($cm^3 \cdot mol^{-1}$)	Δ_P (MPa)
R-32/134a	−1.89	−20.2	0.34
R-32/125	−4.4	−15.81	−0.05
R-125/134a	0.4	−0.85	0.11

Table VIII. Comparisons of Critical Temperatures for R-32/125/134a Mixtures Between Experimental Results and the Proposed Predictive Model, Eq. (14)

Mixture[a]	$T_{c\,exp}$ (K)	$T_{c\,pred}$ (K)	$T_{c\,exp} - T_{c\,pred}$ (K)
R-407A	354.87	354.94	−0.07
NB-A	354.03	354.09	−0.06
NB-B	347.26	347.34	−0.08
R-407C	359.23	358.95	−0.28
R-407E	361.51	361.50	−0.01
NB-C	361.56	361.60	−0.04
Bias			−0.01
SD			0.14

[a] Mixture designations as in Table V.

mixtures. Comparisons between the experimental critical temperatures and the predictive results from Eq. (14) are summarized in Table VIII. Comparisons between experimental critical molar volumes and the predictive results from Eq. (15) are summarized in Table IX. For the critical temperatures of R-32/125/134a mixtures, the predictive results using Eq. (14) are in better agreement with experimental results than the predictive method of Eq. (7). For the critical molar volume, the predictive results of Eq. (15) agree with the experimental data within ±2%. Based on Eqs. (14) and (15), the critical surface of the R-32/125/134a mixture in a temperature–density diagram is shown in Fig. 2.

Table IX. Comparisons of Critical Molar Volumes for R-32/125/134a Mixtures Between Experimental Results and the Proposed Predictive Model, Eq. (15)

Mixture[a]	$V_{c\,exp}$ (K)	$V_{c\,pred}$ (K)	$V_{c\,exp} - V_{c\,pred}$ (K)
R-407A	170.7	174.2	−3.5
NB-A	178.5	175.5	3.0
NB-B	192.3	189.6	2.7
R-407C	170.4	170.0	0.4
R-407E	164.9	167.4	−2.5
NB-C	169.3	164.9	4.4
Bias			−0.73
SD			3.19

[a] Mixture designations as in Table V.

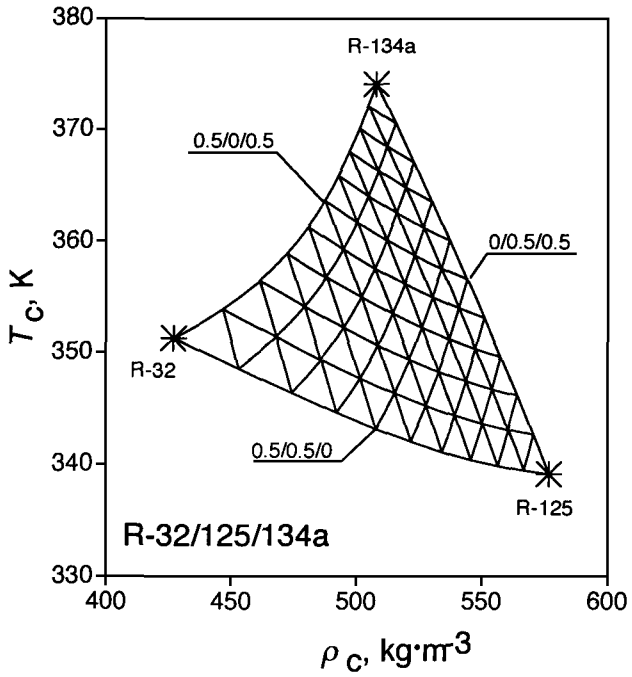

Fig. 2. Critical-point plane for the R-32/125/134a mixtures.

ACKNOWLEDGMENTS

The author is greatly indebted to Asahi Glass Co. Ltd., Tokyo, for kindly furnishing the samples and to T. Ikeda, T. Ishikawa, S. Maruyama, H. Shimizu, and Y. Suzuki, Iwaki Meisei University, for their valuable assistance in this experiment. The author would also like to thank the Physical and Chemical Properties Division, National Institute of Standards and Technology, for the opportunity to work as a Guest Researcher at NIST.

REFERENCES

1. Y. Higashi, *Int. J. Thermophys.* **16**:1175 (1995).
2. Y. Higashi, *J. Chem. Eng. Data* **42**:1269 (1997).
3. Y. Higashi, *J. Chem. Eng. Data* **44**:328 (1999).
4. Y. Higashi, *Int. J. Refrig.* **17**:524 (1994).
5. M. Nagel and K. Bier, *Int. J. Refrig.* **18**:534 (1995).